MOLECULAR AND CELLULAR BIOLOGY, Feb. 2007, p. 1044–1055 Vol. 27, No. 3
0270-7306/07/$08.00+0 doi:10.1128/MCB.01299-06
Copyright © 2007, American Society for Microbiology. All Rights Reserved.

A Novel Plasmid-Based Microarray Screen Identifies Suppressors of *rrp6*Δ in *Saccharomyces cerevisiae*▽†

Katharine Abruzzi,[1]§ Sylvia Denome,[1]§ Jens Raabjerg Olsen,[2]‡ Jannie Assenholt,[2] Line Lindegaard Haaning,[2] Torben Heick Jensen,[2] and Michael Rosbash[1]*

Howard Hughes Medical Institute and Department of Biology, Brandeis University, Waltham, Massachusetts 02454,[1] *and Centre for mRNP Biogenesis and Metabolism, Department of Molecular Biology, Aarhus University, C. F. Møllers Alle, Building 130, 8000 Aarhus C, Denmark*[2]

Received 15 July 2006/Returned for modification 7 August 2006/Accepted 30 October 2006

Genetic screens in *Saccharomyces cerevisiae* provide novel information about interacting genes and pathways. We screened for high-copy-number suppressors of a strain with the gene encoding the nuclear exosome component Rrp6p deleted, with either a traditional plate screen for suppressors of *rrp6*Δ temperature sensitivity or a novel microarray enhancer/suppressor screening (MES) strategy. MES combines DNA microarray technology with high-copy-number plasmid expression in liquid media. The plate screen and MES identified overlapping, but also different, suppressor genes. Only MES identified the novel mRNP protein Nab6p and the tRNA transporter Los1p, which could not have been identified in a traditional plate screen; both genes are toxic when overexpressed in *rrp6*Δ strains at 37°C. Nab6p binds poly(A)$^+$ RNA, and the functions of Nab6p and Los1p suggest that mRNA metabolism and/or protein synthesis are growth rate limiting in *rrp6*Δ strains. Microarray analyses of gene expression in *rrp6*Δ strains and a number of suppressor strains support this hypothesis.

Work, primarily in yeast (*Saccharomyces cerevisiae*), has generated considerable information about the functions of the exosome, a multisubunit complex of proven or predicted 3′-5′ exonucleases. In addition to its role in cytoplasmic-mRNA turnover, the exosome is also involved in a myriad of nuclear events: rRNA, snoRNA, and snRNA processing, as well as the degradation of a variety of stable and unstable nuclear RNAs (1, 2, 4, 12, 16, 27, 28, 34, 36, 44, 45). The nuclear exosome also functions in the surveillance and degradation of aberrant mRNAs/mRNPs and pre-mRNAs (9, 14, 15, 24–26, 31, 41). In its nuclear form, the exosome harbors three specific components, one of which (Rrp6p) has been studied in some detail. An *rrp6*Δ strain grows slowly and is temperature sensitive and deficient in many of the nuclear-RNA-processing and degradation events mentioned above. Importantly, it is not known which of these are most important for the growth defects of the deletion strain.

To address this issue, we identified high-copy-number suppressors of the *rrp6*Δ strain. For more than 2 decades, this strategy has been employed to identify interacting genes and pathways of many different mutant phenotypes in *S. cerevisiae*. Although the approach provides invaluable information, it has stringent requirements. The selection for survival requires a dramatic change in phenotype, i.e., a switch in a life/death discrimination test. The identified genes, therefore, have potent effects, but this suggests that there are probably additional, less potent suppressor genes worth identifying. We therefore also exploited a second approach, which can simultaneously identify enhancer, as well as suppressor, genes, including those that exert much more modest effects on the mutant phenotype. The method, microarray enhancer/suppressor screening (MES), uses DNA microarray technology to rapidly identify genes from plasmid libraries that are either enriched or selected against in a particular test strain during growth in liquid media at normal temperatures. By avoiding high-temperature selection on plates, MES also bypasses interactions with the heat shock pathway. Since an *rrp6*Δ strain is growth impaired in liquid culture at 30°C and grows slowly on plates at 37°C, it is an ideal strain to compare MES with a traditional high-copy-number suppression screen on plates. Moreover, we hoped that the nature of the *rrp6*Δ suppressors might reveal which of the several affected RNA-processing reactions more directly contribute to growth impairment.

We identified five suppressors via MES and two additional suppressors via the traditional plate screen. Five out of the seven identified suppressors either associate with the core exosome (Mtr4p and Dis3p) or are additional 3′-to-5′ exonucleases probably not associated with the exosome (Rex1p to -3p). The remaining two suppressor genes, *LOS1* and *NAB6*, encode the tRNA nuclear export receptor and a novel mRNP binding protein, respectively. We employed Northern blotting analysis and traditional microarray experiments to evaluate the effects of individual suppressors on the RNA population of *rrp6*Δ cells. Based on these data, we propose that mRNA biogenesis and specific protein synthesis are growth limiting in the *rrp6*Δ strain and discuss the mechanisms by which the suppressors may rescue the *rrp6*Δ phenotype.

* Corresponding author. Mailing address: Howard Hughes Medical Institute and Department of Biology, Brandeis University, Waltham, MA 02454. Phone: (781) 736-3160. Fax: (781) 736-3164. E-mail: rosbash@brandeis.edu.

† Supplemental material for this article may be found at http://mcb.asm.org/.

‡ Present address: Interdisciplinary Nanoscience Center iNANO, University of Aarhus, 8000 Aarhus C, Denmark.

§ K.A. and S.D. contributed equally to this work.

▽ Published ahead of print on 13 November 2006.

MATERIALS AND METHODS

Strains and media. All yeast strains used in this study were derived from the W303 background, except as noted in Table S1 in the supplemental material. Standard methods were used for yeast manipulation (22). To create strain SAD11, the *NAB6*-ProtA tag was PCR amplified from pBS1479 (38) with the forward primer 5′-GCCAATATTTTGGGCGCCTCTGCGGAAGACAACAC GCATCCTGACGAGTCCATGGAAAAGAGAAG-3′ and the reverse primer 5′-CTAAATAGTCCGATGGATATGCATTATACTTCAGGCTCAGCACAG CTATATACGACTCACTATAGGG-3′ and integrated.

Library and plasmid construction. Plasmid libraries were constructed with genomic DNA isolated from yeast Δ*cup1*/Δ*crs5* and *rrp6*Δ (Y576) strains. DNA was partially digested with Sau3AI, and 3- to 5-kb fragments were size selected by agarose gel electrophoresis, purified, and inserted into the BamHI site of YEp24 (8). To construct pSAD141-3, the *NAB6* open reading frame (ORF) was PCR amplified from W303 genomic DNA with primers containing SalI and SphI restriction enzyme sites (forward [SalI] primer, 5′-CAGCGTCGACCCTAATG TGCCAA ATACGCTTG; reverse [SphI] primer, 5′-CAGCGCATGCCTTCTG AGCCAAAACTGTCCG), digested, and inserted into the SalI and SphI sites of YEp24. To construct pSAD162-1, the *LOS1* ORF and 5′ and 3′ flanking DNA was PCR amplified from W303 genomic DNA with primers containing BamHI and EagI restriction sites (forward [BamHI] primer, 5′-CAGCGGATCCTGAG AATCTAATGAG TTGTCCCCC; reverse (EagI) primer, 5′-CAGCCGGCCG ATCTTCGTTTGCCTCCCTGC), digested, and inserted into the BamHI and EagI sites of YEp24. To construct pSAD64-5, the *MTR4* ORF and 5′ and 3′ flanking DNA was amplified from wild-type (WT) W303 genomic DNA using primers containing EagI and SphI restriction sites (forward [EagI] primer, 5′-C AGCCGGCCGCAACCTCGGGAAATTCTCGT-3′; reverse [SphI] primer, 5′-CAGCGCATGCCTCCATGTACTGATGTTTGCTTCG-3′). This 4.2-kb fragment was cloned into YEp24 digested with EagI and SphI. To construct pSAD147-1, the *REX2* ORF and 5′ and 3′ flanking DNA was amplified from wild-type W303 genomic DNA using primers containing SalI and SmaI restriction sites (forward [SmaI] primer, 5′-CCCGGGCGTTCCAAGTATTCGTTCA GCGAC-3′; reverse [SalI] primer, 5′-CAGCGTCGACTTGATAATGGAGTC CACTTCAGGG-3′). This fragment was cloned into YEp24 digested with SalI and XmaI. pSADG1 (*RRP6*), pSADG33 (*REX3*), pSADG13 (*REX1*), and pSADG35 (*DIS3*) were from the plate suppressor screen and contained partially Sau3AI-digested genomic DNA from W303 ligated into the BamHI site of YEp24.

Plate suppressor screen. Approximately 5,000 CFU of the *rrp6*Δ strain containing the *cup1*Δ/*crs5*Δ genomic plasmid library was plated onto medium lacking uracil and grown at 37°C for 5 days. Plasmids were isolated from the largest colonies, and inserts were sequenced. Plasmids that were isolated more than once in the screen were retransformed into the *rrp6*Δ strain and retested at 37°C on plates for confirmation of suppression.

Strain growth for MES. The *rrp6*Δ strain was transformed with a YEp24 genomic plasmid library, plated on selective media, and grown at 25°C. After 5 days, colonies were recovered and frozen in 1.5-ml aliquots, each containing 27,000 CFU, representing about 10-fold genomic coverage per aliquot. One 1.5-ml aliquot was used to inoculate 25 ml of yeast synthetic medium lacking uracil with glucose. After 2 h of growth at 25°C, the culture was used to inoculate 200 ml of fresh medium to an A_{600} of 0.01. Cultures were grown at 30°C for 3 days and regularly diluted with prewarmed medium to maintain constant exponential growth. At 0, 24, 48, and 72 h, cell samples were harvested by centrifugation and frozen prior to plasmid isolations. Two independent sets of transformations and growth experiments were performed.

MES probe preparation. Plasmid DNA from each time point was isolated using a yeast plasmid preparation kit (Zymoprep) and amplified through *Escherichia coli* strain DH10B. Passage through bacteria was necessary to generate enough DNA to generate probes. Single-stranded, insert-specific DNA probes were prepared by "linear" PCR (40 cycles) with *Taq* polymerase and one vector-specific primer to incorporate aminoallyl dUTP residues, which were subsequently labeled with either Cy3 or Cy5 monofuctional dye (Amersham). To avoid labeling of the vector DNA, purified plasmid was linearized by restriction enzyme digestion before use. Probes were constructed with either forward- or reverse-directed primers, and Cy3 and Cy5 dyes were switched in duplicate hybridizations to eliminate strand biases. Replicate probes were constructed from two independent growth experiments. For a single growth experiment, at least six microarray probe pairs were prepared: T0 (Cy3) hybridized with T24, T48, and T72 (all Cy5) and T0 (Cy5) hybridized with T24, T48, and T72 (all Cy3). If a particular gene or genomic region was not amenable to PCR, it is possible that it could have been underrepresented in the probe pool. This type of technical difficulty could explain occasional false negatives, such as *MTR4*.

Identification and verification of MES suppressors/enhancers. MES probes were hybridized to yeast Y6.4k microarrays (University Health Network Microarray Centre, Toronto, Canada), following the manufacturer's suggestions. The hybridized microarrays were scanned using a GenePix 4000A (Axon Instruments) scanner, and the data were analyzed in Excel spreadsheet format. Each gene was assigned a rank (1 to 12,437) based on its median ratio of red/green signal (MRAT) value, the data were sorted by the yeast identification number, and gene expression was examined along the chromosomes. Genomic regions where several neighboring genes were highly affected in replicate growth experiments were considered good candidates for PCR verification. This was done by standard PCR amplification (25 cycles) with gene-specific primers and plasmid DNA from the MES pools isolated at 0, 24, 48, and 72 h. PCR products were separated on 1% Tris-acetate-EDTA agarose gels and visualized by ethidium bromide staining. To identify the individual suppressor genes, single ORFs from the genomic regions were PCR amplified from WT genomic DNA and cloned into YEp24. PCR products included approximately 500 bp 5′ and 3′ of the coding sequence. Plasmids containing potential suppressors were transformed into *rrp6*Δ strains with YEp24 as the vector-only control. Cells were grown in uracil$^-$ medium at 25°C to mid-log phase and diluted to an A_{600} of 0.05 in uracil$^-$ medium at 30°C at zero hour. The A_{600} was read every 3 h.

Growth assays on suppressors. The *rrp6*Δ strain was transformed with YEp24 (as the vector-only control) or YEp24 containing a suppressor, including *RRP6*, *NAB6*, *LOS1*, *REX3*, *MTR4*, and *DIS3* (see the details of plasmid construction above). To test growth on plates, cells were grown overnight in medium lacking uracil at 30°C and 10-fold serially diluted; 300-μl aliquots of multiple dilutions were spread onto duplicate plates lacking uracil and grown at 30°C for 2 days or at 37°C for 4 days. To assay growth in liquid at 30°C and 37°C, suppressor-containing *rrp6*Δ cells were grown at either 30°C or 37°C for greater than 12 h to establish steady-state growth at the desired temperature. Once the cells reached steady-state growth and were in early log phase (A_{600} = 0.1), absorbance readings at 600 nm were taken every 2 to 3 h to monitor the growth rate, and the cells were diluted into fresh medium as needed to maintain log-phase growth.

Analysis of rRNA and snoRNA processing. Wild-type, *rrp6*Δ, and suppressor-containing cells were grown to mid-log phase and then shifted to 37°C for 15 min. RNA purification and Northern blotting analysis were performed as previously described (32). To probe for snR38, the radiolabeled DNA oligonucleotide JAS3 was used (GAGAGGTTACCTATTATTACCCATTCAGA CAGGGATAACTG).

The percentage of unprocessed 5.8S rRNA was calculated by dividing the signal from the upper bands by the total signal from 5.8S rRNA species.

Affymetrix microarrays. The wild type (W303 plus YEp24), the *rrp6*Δ strain (*rrp6*Δ plus YEp24), or the *rrp6*Δ strain containing either *RRP6*-YEp24, *MTR4*-YEp24, *REX3*-YEp24, *DIS3*-YEp24, *NAB6*-YEp24, or *LOS1*-YEp24 was grown at either 30°C or 36°C for greater than 12 h to establish steady-state growth. Total RNA was isolated by hot-phenol extraction from 10 ml of cells in late log phase (A_{600} = 1.0). Microarray probes were synthesized and hybridized to Affymetrix Yeast Genome YGS98 arrays according to the manufacturer's specifications. For each strain, microarray analysis was performed on at least three independent RNA samples. All microarrays were analyzed using the statistical program R (http://www.r-project.org) and the bioconductor package (http://www.bioconductor.org; 20). The median value of triplicate microarrays was used in further analysis. Prior to analysis, the data values were transformed into log base 2 in order distribute the data around zero. To analyze the effects of *RRP6* deletion, as well as the suppressors, we divided RNA values from the *rrp6*Δ and *rrp6*Δ suppressor-containing strains with those from the wild-type strain. To examine the effects of growth at 36°C on wild-type, *rrp6*Δ, and *rrp6*Δ plus YEp24-*RRP6* cells, we divided the values obtained at 36°C with those obtained at 30°C.

UV cross-linking assay. UV cross-linking of cells and subsequent isolation of poly(A)$^+$ RNA-containing complexes on oligo(dT) beads was done as previously described (5). Nab6p-TAP fusion protein was detected by Western blotting using protein A-specific antibodies (Sigma).

RESULTS

We first identified high-copy-number suppressors of the temperature-sensitive phenotype of cells with the exosome component, *RRP6*, deleted. *rrp6*Δ cells were transformed with a high-copy-number yeast genomic library and plated at the nonpermissive temperature (37°C). Fast-growing colonies were isolated, and their plasmids were recovered and sequenced. As expected, a large fraction (26%) of the plasmids

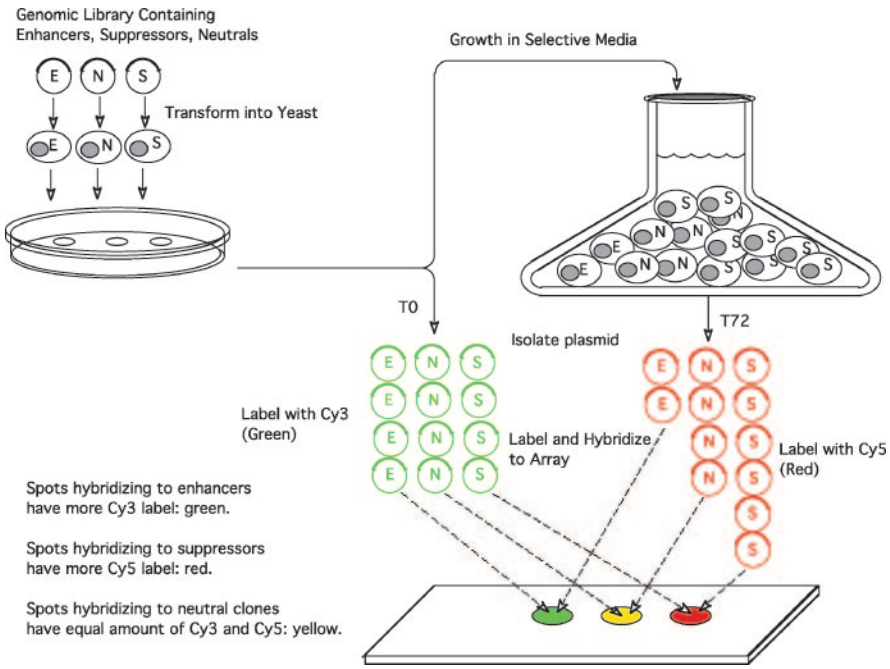

FIG. 1. Schematic representation of MES. The yeast strain of interest is transformed with a plasmid library and plated on appropriate drop-out medium at the permissive temperature. Transformants are recovered and grown in liquid selective medium at the assay temperature. Plasmids improving the growth of the mutant strain are enriched in the population (suppressors); plasmids inhibiting growth of the mutant strain are diminished in the plasmid population (enhancers). At specified time points, plasmid DNA is isolated, labeled with fluorophores, and hybridized to microarrays for identification. In this example, 0-h (T0) plasmids are labeled with Cy3 (shown as green), and the 72-h plasmids are labeled with Cy5 (shown as red). The microarrays are scanned, the MRAT for each gene is determined, and the genes are ranked from highest to lowest MRAT (the highest MRAT is given a value of 1). Spots that have high MRAT rankings are green, indicating that the gene is more highly abundant in the T0 plasmid population (enhancers). Spots that are red have low MRAT rankings, because the gene is more highly abundant in the T72 population (suppressors). Yellow spots are equally abundant in both plasmid populations.

contained the *RRP6* gene (data not shown). In addition, we identified extragenic suppressor-containing plasmids, including four groups of overlapping fragments, each of which contained a single "exosome-relevant" gene: *DIS3*, *MTR4*, *REX1*, or *REX3*. All four of these suppressors were verified to have biological activity; single ORFs with flanking DNA rescued the growth defect of *rrp6*Δ (see Materials and Methods). Moreover, the activities of all four suppressors can be easily rationalized. Dis3p, related to the 3′ hydrolases RNase II and RNase R from *E. coli*, is an exosome component or associates with the exosome (3), and the helicase Mtr4p is an exosome cofactor (17, 30, 42). The overexpression of these two genes may stimulate the endogenous Rrp6p-lacking nuclear exosome or perhaps mitigate exosome instability in the absence of Rrp6p. *REX1* and *REX3* both encode 3′→5′ exonucleases (43). High-copy-number expression of these genes presumably complements the deficient 3′-to-5′ exonucleolytic activities of the *rrp6*Δ background.

To identify additional *rrp6*Δ suppressors not dependent on a traditional plate high-temperature rescue strategy, we turned to our new MES methodology (Fig. 1). In brief, the same high-copy-number genomic-DNA library—or a similar library made from *rrp6*Δ genomic DNA—was used to transform the *rrp6*Δ strain at 25°C. The entire transformation was then inoculated into liquid culture and grown at 30°C, keeping the culture in exponential growth by repetitive dilution. We hypothesized that plasmids containing suppressors would stimulate cell growth and become enriched in the population. In contrast, plasmids containing enhancers would cause the cells to grow more slowly and would consequently decrease in the population. Cells were collected and frozen at the time of inoculation (0 h) and then after 24, 48, and 72 h of growth. Plasmid DNA was isolated from cells at each time point, and microarray probes were prepared from the inserts. Probes from the 0-h time point (made with one fluorophore, e.g., green) and a later time point (either 24, 48, or 72 h; made with the other fluorophore, e.g., red) were mixed and hybridized to cDNA microarrays, which monitored changes in the plasmid population over time. The genes were ranked by MRAT, the results were examined for genomic regions in which several neighboring genes were similarly ranked (high or low in abundance; see Materials and Methods), and both potential suppressors and enhancers were identified. Further testing revealed that most of the enhancers were not specific, i.e., they caused slow growth in a variety of genetic backgrounds, dictating a focus on the suppressors.

RRP6 and its chromosomal neighbors were easily detectable as suppressors in the MES analysis (Fig. 2A). Multiple genes in this cluster were ranked in the top 0.1% of genes, i.e., with MRAT rankings of less than 12. *RRP6* was such a strong suppressor that the cluster containing *RRP6* was already highly abundant by 24 h, resulting in little or no change in ranking over time. We also identified a number of candidate extragenic suppressor regions. The rankings for two representative re-

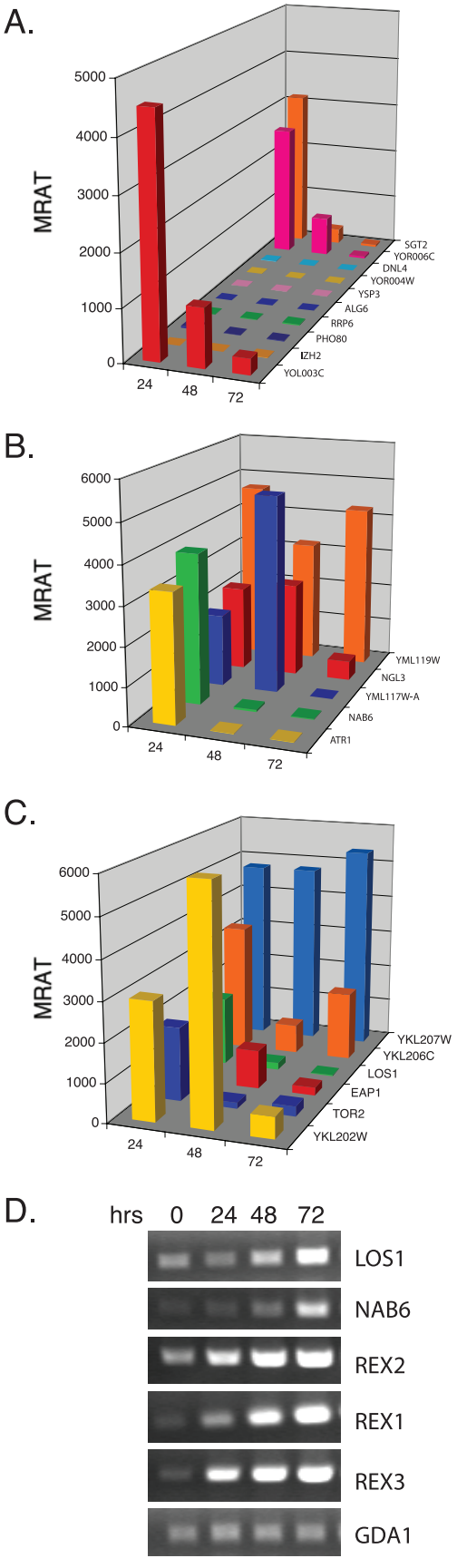

TABLE 1. Summary of *rrp6*Δ suppressors

Gene	Method of identification	Suppresses at[a]:	
		30°C	37°C
DIS3	Plate	−	+
LOS1	MES	+	−
MTR4	Plate	+	+
NAB6	MES	+	−
REX1	Both	+	+
REX2	MES	+	+
REX3	Both	+	+

[a] +, suppression; −, no suppression.

gions are shown (Fig. 2B and C). They included the *NAB6* gene, which encodes a putative mRNA binding protein (40), and the *LOS1* gene, which encodes a tRNA binding protein involved in tRNA export from the nucleus (21). Both of these suppressors became enriched in the plasmid population over time (with progressively lower MRAT rankings from 24 to 72 h of growth). Three additional extragenic suppressor regions contained the genes encoding the 3′-5′ exonucleases, *REX1*, *REX2*, and *REX3* (data not shown). Only two of these five genes (*REX1* and *REX3*) were also identified in the plate suppressor screen (Table 1). Each of these suppressor regions was validated by MES analyses from two independent growth experiments and was confirmed by PCR for enrichment of the extragenic suppressor regions throughout the time course (Fig. 2D). The candidate gene was then subcloned and shown to partially rescue the growth defects of the *rrp6*Δ strain at 30°C (Fig. 3A) (see below). All five genes were confirmed by all criteria.

Characterization of the *rrp6*Δ suppressors. The MES and traditional plate screening were done in the same strain back-

FIG. 2. Identification and verification of suppressors of *rrp6*Δ in liquid culture. The MES method was carried out using the *rrp6*Δ strain. Plasmid DNA isolated at 0, 24, 48, and 72 h was used to construct probes. Microarray probes produced for all later time points (24, 48, and 72 h) were hybridized against probes from the zero time point. The genes are ranked by the MRAT value, with the best suppressor assigned rank 1. Because a genomic library was used in the screen, the candidate suppressor and neighboring genes are enriched in the population. (A) MRAT rankings over time for the region of chromosome 15 containing *RRP6* and its neighboring genes. *RRP6* (green) and a cluster of surrounding genes are highly enriched in the plasmid population, i.e., they have very low MRAT rankings even by 24 h. (B) MRAT rankings over time for the region of chromosome 13 containing *NAB6* and its neighboring genes. Note that the *NAB6* gene (shown in green) and some of the neighboring genes increased in rank (i.e., have lower MRAT rankings) over time from 24 to 72 h, which indicates that plasmids containing these genes became more prevalent in the population. (C) MRAT rankings over time for a region of chromosome 11 containing *LOS1* and its neighboring genes. The *LOS1* gene (in green) or the neighboring genes had lower MRAT rankings over time, indicating that plasmids containing these genes became more prevalent in the population. (D) Confirmation of MES suppressors *LOS1*, *NAB6*, *REX1*, *REX2*, and *REX3*. *rrp6*Δ cells transformed with the *rrp6*Δ genomic plasmid library were harvested after 0, 24, 48, and 72 h of growth at 30°C. PCR amplification using gene-specific primers revealed plasmid enrichment over time. The products were separated by electrophoresis on 1% agarose and visualized by ethidium bromide staining. *GDA1* was included as a negative control.

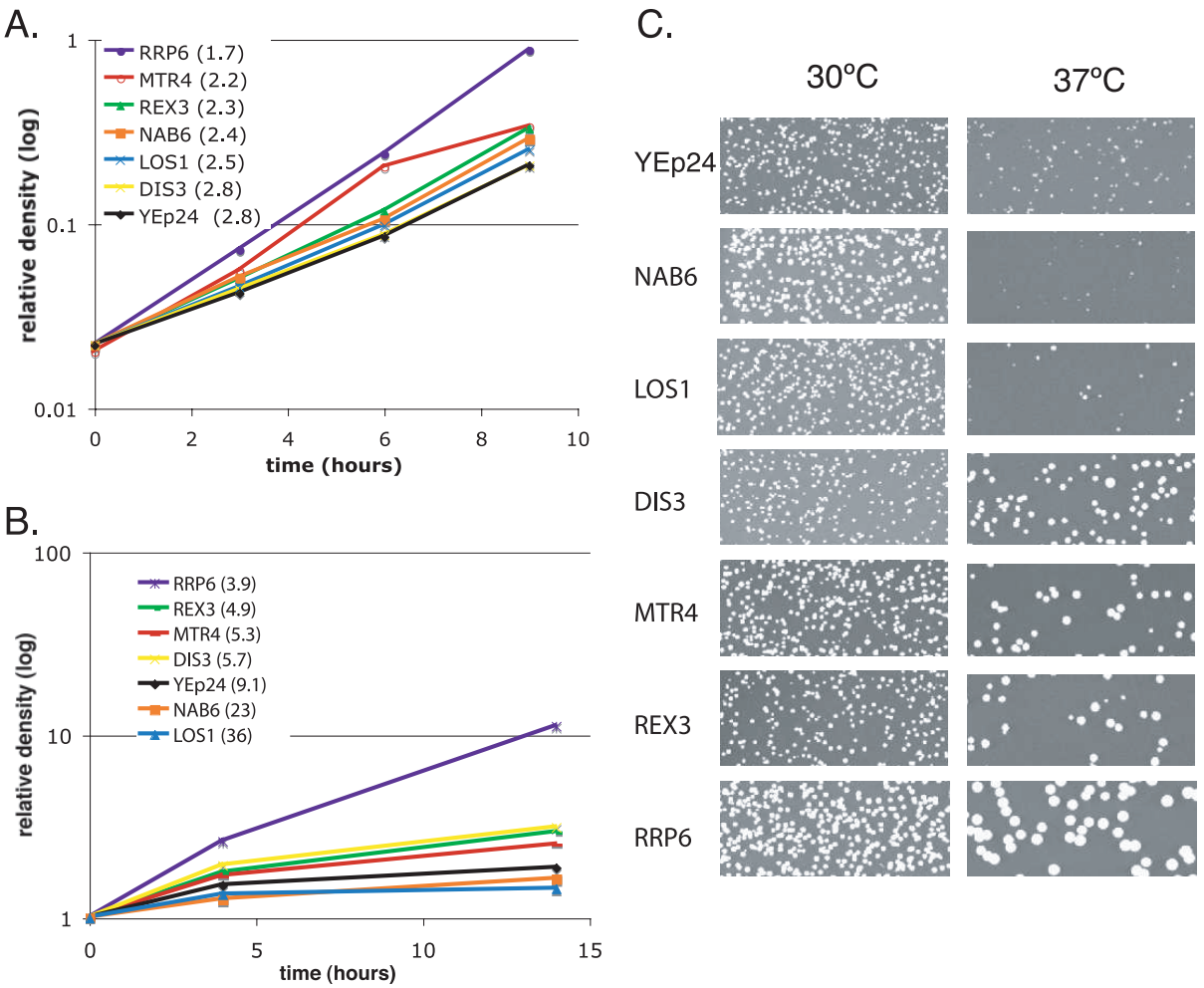

FIG. 3. Abilities of suppressors to rescue the growth defects of the *rrp6*Δ strain at 30°C and 37°C. The *rrp6*Δ strain was transformed with YEp24, pYEp24-*RRP6*, pYEp24-*NAB6*, pYEp24-*LOS1*, pYEp24-*DIS3*, pYEp24-*MTR4*, and pYEp24-*REX3*. The doubling time of each strain is presented in the graph legend. The *rrp6*Δ cells overexpressing *RRP6* had a growth rate nearly identical to that of the wild-type cells. (A) Transformants were grown in medium lacking uracil at 30°C (see Materials and Methods). Cell growth was monitored by reading the A_{600} every 2 to 3 h. The overexpression of *NAB6*, *LOS1*, *MTR4*, and *REX3* improved the growth of the *rrp6*Δ strain, whereas *DIS3* had no effect. (B) Transformants were grown in medium lacking uracil at 37°C until they reached early log phase (see Materials and Methods). Cell growth was monitored by reading the A_{600} every 2 to 3 h. At 37°C, the overexpression of *DIS3*, *REX3*, and *MTR4* rescued the growth of the *rrp6*Δ strain. Unlike at 30°C, *NAB6* and *LOS1* overexpression did not rescue the growth of the *rrp6*Δ strain. (C) Transformants were plated on medium lacking uracil and grown at either 30°C or 37°C for 2 or 4 days, respectively. At 30°C, it was hard to detect any differences in growth between the control and the suppressor-containing cells. At 37°C, the overexpression of *DIS3*, *MTR4*, and *REX3* substantially rescued the growth defects of the *rrp6*Δ strain. In contrast, *NAB6* and *LOS1* overexpression did not rescue the *rrp6*Δ strain growth defects and were actually toxic to *rrp6*Δ cells (less than 0.2% of the plated cells formed colonies).

ground with the same high-copy-number genomic library, yet the two approaches identified slightly different genes (Table 1). These differences could be due to temperature (30°C versus 37°C), to the growth environment (i.e., liquid versus plate), or to modest technical variations. To learn more about both sets of suppressors, we transformed the *rrp6*Δ strain with high-copy-number plasmids expressing *RRP6*, *NAB6*, *LOS1*, *MTR4*, *DIS3*, or *REX3*. We examined the growth of these suppressor-containing strains, as well as the *rrp6*Δ strain containing an empty vector control (YEp24), under steady-state conditions at 30°C and 37°C, both on plates and in liquid media (Fig. 3).

Interestingly, the suppressors showed substantial differences in their abilities to suppress the *rrp6*Δ defects at 30°C and 37°C. YEp24-*NAB6*, YEp24-*LOS1*, YEp24-*MTR4*, and YEp24-*REX3* partially rescued the growth defects of *rrp6*Δ cells at 30°C in liquid (Fig. 3A; note the log scale, as well as the doubling times in the graph). Overexpression of *DIS3* at 30°C did not rescue the *rrp6*Δ strain growth defect and made wild-type cells slightly sick (with a 20% increase in doubling time [data not shown]). This suggests that any growth advantage of *DIS3* at 30°C might have been be masked by toxicity. It is harder to know whether the suppressors affected plate growth at 30°C, because there was only a slight size difference between wild-type (YEp24-*RRP6*) and mutant colonies at this temperature (Fig. 3C).

At 37°C, overexpression of *MTR4*, *DIS3*, and *REX3* improved the growth rate of the *rrp6*Δ strain both on plates and in liquid (Fig. 3B and C). In contrast, *LOS1* and *NAB6* over-

expression had the opposite effect; they are enhancers of the *rrp6*Δ strain growth defect at 37°C, both in liquid (with doubling times of >23 h) and on plates. Overexpression of *NAB6* and *LOS1* not only caused cells to become slow growing but also led to a loss of viability (<0.2% of cells formed colonies at 37°C) (data not shown).

The abilities of the various genes to suppress or enhance the growth defects of the *rrp6*Δ strain were specific; none of them rescued the growth defects of a temperature-sensitive actin-related protein (*arp2-1*) (35) under identical conditions, and overexpression of *LOS1* and *NAB6* at high temperature had no effect on the growth of a wild-type strain (data not shown). The results underscore the utility of the MES approach and suggest that *NAB6* and *LOS1* would not have been identified in traditional plate screens, because they are toxic to the *rrp6*Δ strain at high temperatures and are difficult to score on plates at 30°C.

Suppressors of *rrp6*Δ do not restore 5.8S rRNA or snoRNA processing. 5.8S rRNA and some snoRNAs are well-examined substrates of Rrp6p/exosome maturation activity (1, 10, 19, 44). It is possible that the various suppressors partially rescue the slow growth of *rrp6*Δ cells simply by restoring proper processing of such "bona fide" Rrp6p substrates. To test this hypothesis, we examined 5.8S rRNA and snoRNA (snR38) maturation after a 15-min shift to 37°C in wild-type (W303 plus YEp24), *rrp6*Δ (*rrp6*Δ plusYEp24), and *rrp6*Δ suppressor-containing (*rrp6*Δ containing the various suppressors) cells.

As previously reported, a deletion of *RRP6* causes the accumulation of both 5.8S rRNA- and snoRNA-processing intermediates (10, 18, 33, 44) (Fig. 4A). These intermediates were barely detectable in both the wild-type strain and the *rrp6*Δ strain containing YEp24-*RRP6*. Rex2p overexpression in *rrp6*Δ cells resulted in an almost complete rescue of unprocessed 5.8S rRNA and snR38 (Fig. 4A and B). In contrast, neither of the other suppressors had any effect. Identical results were obtained under steady-state growth conditions at 30°C (data not shown). Thus, the mechanism of *rrp6*Δ growth suppression of Rex1p, Rex3p, Mtr4p, Dis3p, Los1p, and Nab6p is almost certainly not due to restoration of proper 5.8S rRNA and snoRNA processing.

Effects of *RRP6* and its suppressors on RNA levels at 30°C. Because most of the suppressors could not be explained by a simple restoration of candidate stable RNA processing, we turned to standard microarray gene expression analyses. We first characterized the overall RNA profile of an *rrp6*Δ strain (*rrp6*Δ plus YEp24) grown at 30°C. The *rrp6*Δ strain RNA levels were compared to those of a wild-type strain (WT plus YEp24 vector), and the RNA levels are presented as the difference relative to the wild type (Fig. 5). Previous studies have shown that there are dramatic increases in polyadenylated rRNA, snRNAs, snoRNAs, tRNAs, and so-called CUTs (cryptic unstable transcripts) when *RRP6* is deleted (1, 16, 27, 29, 44, 45). The fact that a *TRF4*- or *TRF5*-encoded poly(A) polymerase acts upstream of the nuclear exosome to identify improperly processed RNAs or CUTs for degradation explains these observations: weak exosome activity increases the levels of these polyadenylated degradation intermediates, which are then visible because of the standard Affymetrix oligo(dT) cDNA-priming protocol (27, 30, 42, 45). To analyze the effect of an *RRP6* deletion on different classes of noncoding RNAs,

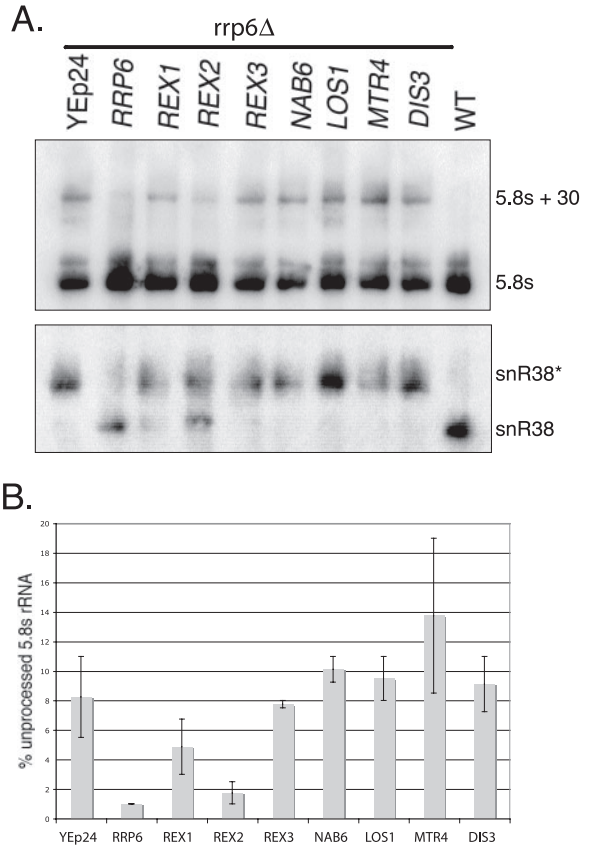

FIG. 4. Effects of suppressors on 5.8S rRNA and snoRNA processing. RNA was isolated from wild-type cells and *rrp6*Δ cells containing either an empty YEp24 vector, YEp24-*RRP6*, YEp24-*REX1*, YEp24-*REX2*, YEp24-*REX3*, YEp24-*NAB6*, YEp24-*LOS1*, YEp24-*MTR4*, or YEp24-*DIS3*. (A) RNA was analyzed by Northern blotting with radiolabeled probes for either 5.8S RNA or snR38 (see Materials and Methods for details). When *RRP6* was deleted, both 5.8S rRNA (5.8S + 30) and snR38 (snR38*) processing intermediates were visible (compare YEp24 with WT). Overexpression of *RRP6* and *REX2* substantially reduced the levels of both 5.8S rRNA and snoRNA processing intermediates. (B) Quantitation of the abilities of the suppressors to restore proper 5.8S rRNA processing. The amount of 5.8S + 30 rRNA was divided by the total amount of 5.8S rRNA in each suppressor-containing strain. The average of two independent experiments is presented, and standard deviation is represented by error bars.

we used the median expression value for an entire RNA class as a benchmark. In addition, we examined the effect on the entire poly(A) rRNA population (total rRNA), as well as each individual rRNA subclass (5S, 37S, 25S, and 18S). As expected, there were significant increases in poly(A) rRNA, snRNAs, snoRNAs, tRNAs, and CUTs in the *rrp6*Δ strain (Fig. 5).

There are also mRNAs that are down- as well as up-regulated in the *rrp6*Δ strain at 30°C; 11 mRNAs were down-regulated 10-fold or more, and 3 mRNAs were up-regulated 10-fold or more (data not shown; see Table S2 in the supplemental material). Although mRNA down-regulation has not been verified by independent assays, signals were low compared to both a WT strain and the *rrp6*Δ strain rescued with high-copy-number *RRP6* (data not shown). Moreover, a similar number of mRNAs were reported to be down-regulated in *rrp6*Δ cells in a previous study (23). Note that *RRP6* itself is the

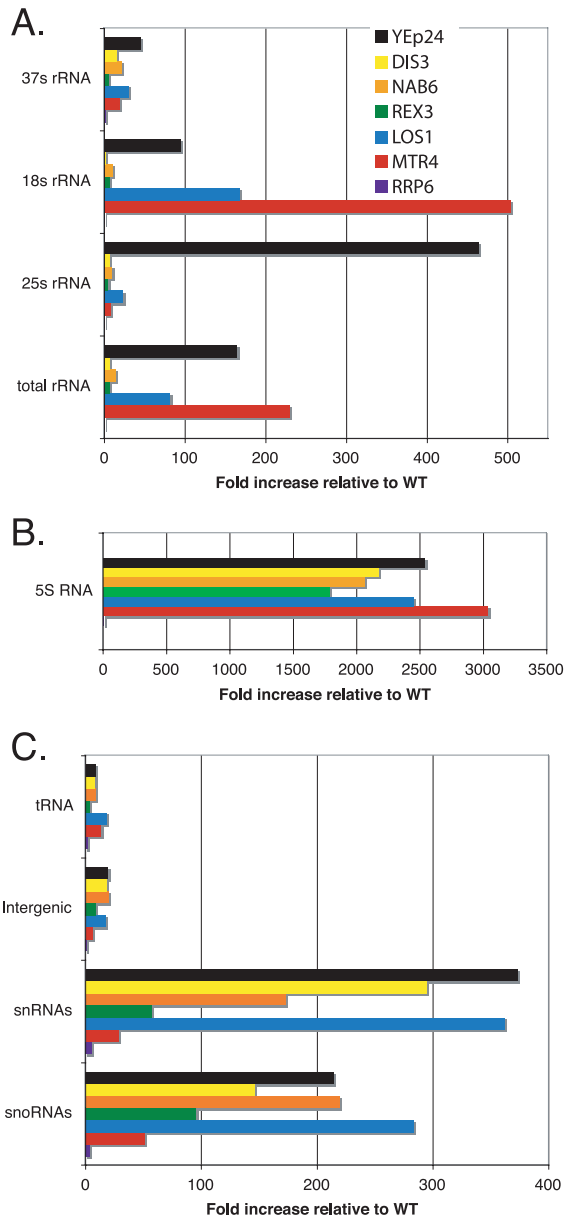

FIG. 5. Polyadenylated stable RNAs in the *rrp6*Δ strain at 30°C. Affymetrix microarrays were used to examine the levels of poly(A)-stable RNAs in WT cells and in the *rrp6*Δ strain containing either an empty YEp24 vector (black), YEp24-*DIS3* (yellow), YEp24-*NAB6* (orange), YEp24-*REX3* (green), YEp24-*LOS1* (blue), YEp24-*MTR4* (red), or YEp24-*RRP6* (purple). The RNA levels in the *rrp6*Δ strains were normalized relative to the wild-type strain and are presented as the increase relative to the WT. (A and B) The relative levels of poly(A) rRNAs that accumulate in *rrp6*Δ cells containing either an empty YEp24 plasmid (black) or YEp24-suppressor plasmids. The levels of poly(A) 37S, 18S, 25S, and 5S rRNAs increased when *RRP6* was deleted, and these levels were reduced by a subset of the suppressors. For rRNA classes with multiple Affymetrix probes, the median value was used. (C) Relative levels of poly(A) tRNAs, snRNAs, snoRNAs, and CUTs that accumulated in *rrp6*Δ cells containing either an empty YEp24 plasmid (black) or YEp24-suppressor plasmids. Deletion of *RRP6* resulted in an increase in poly(A)-stable RNAs whose levels were modulated by the supressors.

most down-regulated probe set, because of the gene deletion (see Table S2 in the supplemental material).

To analyze suppressor effects on the RNA population in the *rrp6*Δ strain at 30°C, we normalized microarray data from the suppressor strains relative to the WT and compared these values to similar data from the *rrp6*Δ strain (Fig. 5). All of the suppressors lowered the levels of poly(A) 37S and 25S rRNAs, and *REX3*, *DIS3*, and *NAB6* partially rescued 18S rRNA levels (Fig. 5A; compare the colored bars to the black bars). Interestingly, none of the suppressors had a strong effect on the dramatic increase in poly(A) 5S RNA (Fig. 5B). The abilities of all of the suppressors to reduce the levels of some poly(A) rRNA species suggest that these effects may be indirect, i.e., the increase in the growth rate may lead to a decrease in some poly(A) rRNAs. However, it is important to note that Dis3p lowers poly(A) rRNA levels even without affecting the growth rate.

The levels of poly(A) tRNAs, CUTs, snRNAs, and snoRNAs were reduced by only a subset of the suppressors (Fig. 5C). Both Mtr4p and Rex3p substantially lowered the levels of poly(A) CUTs, snRNAs, and snoRNAs, whereas only Rex3p overexpression affected tRNA levels (Fig. 5C). Dis3p overexpression slightly decreased the levels of snRNAs and snoRNAs. Nab6p overexpression reduced the amount of poly(A) snRNAs by about twofold, and Los1p overexpression did not lower the levels of any of the poly(A)-stable RNAs. The fact that *MTR4*, *DIS3*, and *REX3* differentially affected the different stable RNA classes (compare the yellow, red, and green bars in Fig. 5) suggests that each of these exonucleases or exosome cofactors preferentially processes or degrades specific noncoding RNAs.

The suppressors also restored the mRNA levels of several genes that were substantially down-regulated in the *rrp6*Δ strain. For example, 3 of the 11 most down-regulated mRNAs in the *rrp6*Δ strain are *COS7*, *YVC1*, and YBR074W (see Table S2 in the supplemental material). The expression of each of these genes was up-regulated approximately 2- to 15-fold by all the growth-restoring suppressors, but not by the only suppressor that did not rescue growth at 30°C, *DIS3*. This indicates that either the growth-restoring suppressors all impact a common set of mRNAs or the levels of some mRNAs are due to slow growth and increase with an improved growth rate.

Suppression by *NAB6* is likely linked to mRNA metabolism. Nab6p has sequence characteristics of an mRNA-binding protein (40). Indeed, protein-A-tagged Nab6p can be UV cross-linked in vivo to polyadenylated RNA in a wild-type strain (Fig. 6) (5). Furthermore, genetic experiments show that a deletion of *NAB6* partially rescues the growth defects of two mutants involved in 3′-end formation: *rna14-3* and *pcf11-2* (data not shown). Based on these properties, we looked for mRNAs preferentially up-regulated by *NAB6* overexpression in the *rrp6*Δ strain (i.e., we divided the levels of RNAs in *rrp6*Δ plus *NAB6* by the levels in *rrp6*Δ plus YEp24). The mRNAs that are most up-regulated by Nab6p overexpression are shown in Table 2; as expected, the top probe set is *NAB6*. In this set, we looked for mRNAs down-regulated in the *rrp6*Δ strain whose up-regulation upon *NAB6* overexpression was unlikely to be due to an increase in the growth rate, i.e., mRNAs unaffected by other growth-restoring suppressors (Table 2). Several transcripts were up-regulated three- to fivefold, includ-

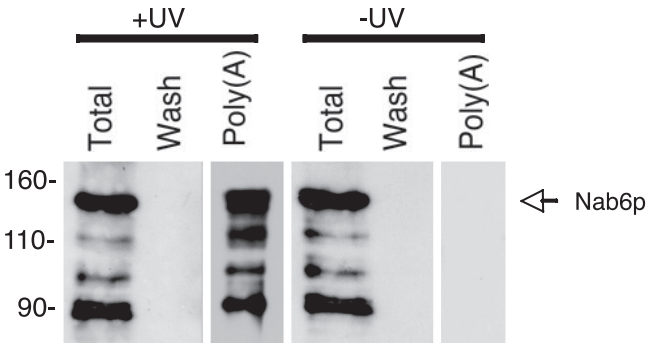

FIG. 6. Nab6p binds to poly(A) RNA. (A) Cells expressing Nab6-TAP as the only source of Nab6p were treated with (+UV) or without (−UV) UV cross-linking in vivo. Subsequently, poly(A)$^+$ RNA was purified on oligo(dT)-cellulose columns and treated with RNase prior to analysis by Western blotting for the presence of Nab6-TAP. In control experiments, the poly(A)$^+$ RNA fractions were also analyzed for the presence of Npl3p and Nop1p; as previously reported, Npl3p binds and Nop1 does not bind poly(A)$^+$ RNA (39) (data not shown).

ing mRNAs from the *RAD51*, *RIM4*, *MTL1*, *GYP5*, *SUL1*, and *NAM8* genes. Interestingly, mRNAs from the *RAD51*, *MTL1*, *SUL1*, and *NAM8* genes are also two- to fourfold up-regulated by *NAB6* overexpression in a wild-type background (data not shown). The effect of *NAB6* overexpression on *RAD51* and *NAM8* mRNAs in both backgrounds has been verified by quantitative PCR (data not shown). These results suggest that *NAB6* rescues the growth defect of the *rrp6*Δ strain by stabilizing a specific subset of mRNAs.

Effect of *rrp6*Δ on RNA levels during steady-state growth at 36°C. Cells with *RRP6* deleted grow much more slowly at 37°C than at 30°C (doubling times, 9.1 h versus 2.8 h, respectively). To study this effect and to try to understand why *NAB6* and *LOS1* overexpression is toxic to *rrp6*Δ cells at high temperature, we performed microarray analysis after growing cells at high temperature. Because *rrp6*Δ cells grow somewhat faster at 36°C (doubling time, 7 h), we thought that this temperature might reduce the indirect effects on gene expression of even slower growth at 37°C. Importantly, the overexpression of both *LOS1* and *NAB6* was toxic at 36°C, as well as at 37°C; i.e., there was a further decrease in the growth rate at both temperatures (data not shown).

To determine the effects of the higher temperature, we first compared the RNA profiles generated from wild-type (wild type plus YEp24), *rrp6*Δ (*rrp6*Δ plus YEp24), and *rrp6*Δ plus YEp24-*RRP6* cells grown at 30°C and 36°C. In all three strains, the levels of poly(A) rRNAs, tRNAs, CUTs, snRNAs, and snoRNAs all increased at least twofold when grown at 36°C (Fig. 7A and B). Poly(A) 5S RNAs are dramatically up-regulated in both wild-type and Rrp6p-overexpressing cells upon the shift to 36°C: 400-fold and 950-fold, respectively (data not shown). In *rrp6*Δ cells, in contrast, poly(A) 5S RNA levels

TABLE 2. *NAB6* overexpression restores mRNAs that are down-regulated in the *rrp6*Δ strain at 30°C[a]

Transcript identifier[b]	Gene	Change in mRNA levels (*n*-fold)[c]					
		*rrp6*Δ/WT	*NAB6*/*WT*	*DIS3*/WT	*REX3*/WT	*MTR4*/WT	*LOS1*/WT
YML117W	*NAB6*	2.09	49.58	1.03	0.88	2.28	1.01
YBR076W	*ECM8*	9.91	34.30	12.08	11.18	4.22	13.76
YBL048W		2.28	9.66	0.86	2.03	1.21	3.41
YOR387C		2.31	8.98	1.56	3.97	1.26	0.10
YOR049C	*RSB1*	1.53	6.37	3.10	2.50	0.43	2.44
YER095W	*RAD51*	0.86	4.86	0.72	1.06	0.59	1.27
YNL017C		1.42	4.66	1.52	1.10	0.99	1.70
YAL067C	*SEO1*	1.00	4.11	0.42	4.26	1.65	1.04
YOR008C-A		1.24	4.09	1.20	0.98	0.71	0.88
YOR178C	*GAC1*	1.07	3.66	0.30	0.62	0.68	2.23
YDR076W	*RAD55*	1.05	3.16	0.92	1.12	0.84	1.08
YGR023W	*MTL1*	0.71	3.07	0.48	1.53	1.13	1.43
YHL024W	*RIM4*	0.60	2.81	0.23	1.24	0.76	1.19
YBR294W	*SUL1*	0.88	2.79	0.77	1.23	0.52	1.23
YGL258W		0.46	2.03	0.68	2.72	0.39	0.19
YHR086W	*NAM8*	0.53	1.70	0.45	0.81	0.54	1.05
YBR132C	*AGP2*	0.46	1.70	0.27	1.16	0.73	1.13
YDR255C	*RMD5*	0.48	1.57	0.42	1.01	1.22	1.00
YOR302W		0.22	1.12	0.03	1.71	2.65	1.37
YGL259W	*YPS5*	0.13	1.00	0.07	0.98	1.23	1.02
YMR140W	*SIP5*	0.31	0.99	0.17	0.89	2.73	0.91
YEL065W	*SIT1*	0.24	0.93	0.39	0.84	0.44	0.40
YDL248W	*COS7*	0.08	0.82	0.06	1.58	1.48	0.70
YOR087W	*YVC1*	0.11	0.80	0.03	1.13	1.54	0.70
YMR058W	*FET3*	0.12	0.65	0.33	1.03	0.16	0.11
YIL141W		0.20	0.64	0.13	1.11	5.02	0.79
YLR162W		0.10	0.62	0.13	2.03	0.19	0.18
YPL249C	*GYP5*	0.15	0.58	0.19	0.28	0.13	0.29
YJL153C	*INO1*	0.06	0.18	0.01	0.06	0.19	0.06

[a] The table lists the mRNAs that are most up-regulated by *NAB6* overexpression in the *rrp6*Δ strain (*rrp6*Δ plus *NAB6* divided by *rrp6*Δ plus YEp24).
[b] Boldface indicates mRNAs that are down-regulated in the *rrp6*Δ strain and specifically up-regulated by *NAB6* overexpression, i.e., they are less affected by the other suppressors.
[c] Difference in mRNA levels in the *rrp6*Δ and *rrp6*Δ strains overexpressing *NAB6*, *DI53*, *MTR4*, or *LOS1*, all relative to wild type.

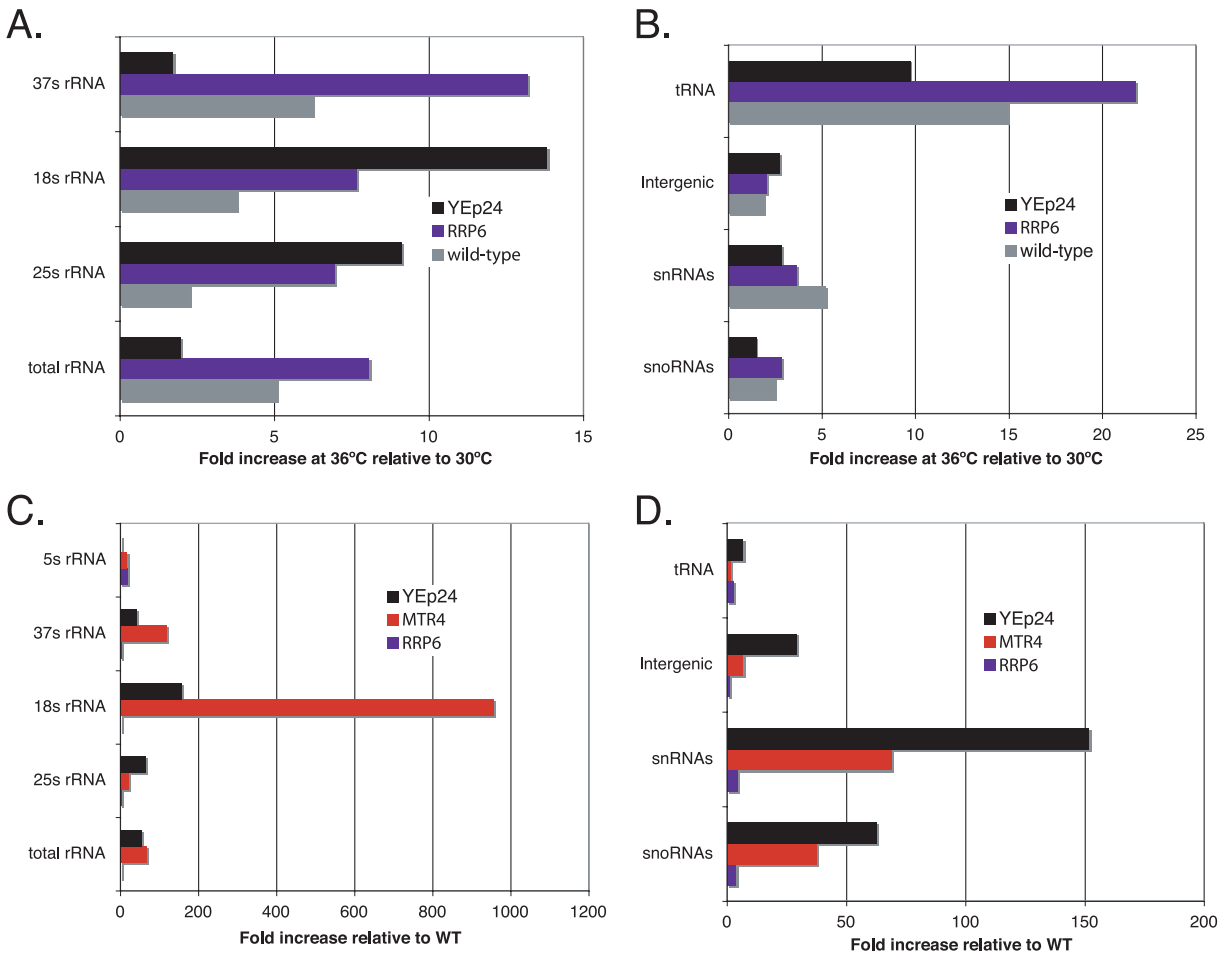

FIG. 7. Polyadenylated stable RNAs in the *rrp6*Δ strain at 36°C. Affymetrix microarrays were used to examine the levels of poly(A)-stable RNAs that accumulated during steady-state growth at 36°C. RNA from wild-type (gray) or *rrp6*Δ cells containing an empty YEp24 vector (black), YEp24-*RRP6* (purple), or YEp24-MTR4 (red) was isolated. (A and B) RNA levels from steady-state growth at 36°C were normalized relative to RNA levels from the same strains grown at 30°C. The graphs show the increase in the levels of poly(A)-stable RNAs resulting from steady-state growth at 36°C. (C and D) RNA levels from *rrp6*Δ strains containing either YEp24, YEp24-*RRP6*, or YEp24-*MTR4* grown at 36°C were normalized to RNA levels of wild-type cells grown at 36°C. Deletion of *RRP6* caused an increase in the levels of poly(A) rRNA, tRNAs, CUTs, snRNAs, and snoRNAs at 36°C (black bars). Overexpressing *RRP6* (purple bars) and *MTR4* (red bars) can suppress the accumulation of a subset of these poly(A)-stable RNAs.

actually decrease upon a shift to 36°C; however, levels are still twofold higher than those from the wild-type strain (data not shown). These observations suggest that growth at 36°C may cause defects in tRNA, snRNA, snoRNA, and rRNA processing, which lead to their identification and polyadenylation by the Trf4p pathway.

To determine the effects of the *RRP6* deletion, we compared *rrp6*Δ strain RNA levels at 36°C to those from a wild-type strain grown at the same temperature (Fig. 7C and D). As observed at 30°C, there was an increase in poly(A) tRNAs, snRNAs, snoRNAs, CUTs, and some rRNAs at 36°C (Fig. 7C and D). The magnitude of the effect at 36°C was not as high as at 30°C, however, due in part to the already elevated levels of poly(A)-stable RNAs in the wild-type background at 36°C (see above) (Fig. 7A and B).

Deletion of *RRP6* more dramatically affects mRNA levels when cells are grown at 36°C. Six hundred eight mRNAs were down-regulated greater than 10-fold, whereas only 83 mRNAs were up-regulated more than 10-fold relative to wild-type cells at 36°C (Table 3 and data not shown). The down-regulated mRNAs include a number of factors involved in mRNA metabolism, such as 18 transcription factors, the DEAD box RNA helicase Dbp2p, the mRNA export factor Mex67p, and the mRNA surveillance factor Mlp1p. It is possible that the *RRP6* deletion more directly affects the levels of a subset of these RNA metabolism mRNAs and encoded proteins, which then cause decreases in a larger set of mRNAs.

MTR4 overexpression significantly rescues the growth defects of the *rrp6*Δ strain at 36°C, from a doubling time of approximately 7 h to 3.3 h. To learn more about how *MTR4* overexpression rescues the *rrp6*Δ strain at 36°C, we examined the RNA profiles of *rrp6*Δ cells overexpressing *MTR4* grown at this temperature. The data are normalized to those from a wild-type strain grown at the same temperature, and they are presented side by side and compared with similar data from an *rrp6*Δ strain (Fig. 7C and D). Overexpression of *MTR4* had

TABLE 3. Down-regulated mRNAs that are not restored by *MTR4* overexpression

Gene	Downregulation (*n*-fold)	
	YEp24/WT	*MTR4*/WT
CTS1	0.002	0.016
HCR1	0.002	0.02
VMA6	0.003	0.022
IKI3	0.004	0.009
ADE16	0.004	0.02
SHM2	0.004	0.003
RPL15A	0.007	0.04
ZPS1	0.007	0.009
AUR1	0.01	0.05
GMH1	0.01	0.03
MMM1	0.01	0.04
SBA1	0.01	0.03
LAS1	0.02	0.01
MLP1	0.02	0.02
PRP19	0.02	0.07
TUL1	0.02	0.03
VPH2	0.03	0.008
SAP190	0.03	0.03
NMT1	0.03	0.07
AAT2	0.04	0.015
IFH1	0.04	0.04
TRP3	0.05	0.012
UBA1	0.06	0.04
RPC25	0.06	0.04
ZRT3	0.08	0.008
ORM2	0.08	0.04
ADH4	0.08	0.07
UTP13	0.08	0.04
LST4	0.1	0.09

slightly different effects on poly(A)-stable RNAs at 36°C than at 30°C. As observed at 30°C, *MTR4* overexpression reduced the levels of poly(A) snRNA, snoRNAs, CUTs, and 25S rRNA and increased the levels of poly(A) 18S RNA (Fig. 7B and C; compare the black and red bars). However, at 36°C, MTR4 reduced the levels of poly(A) tRNAs and increased the levels of poly(A) 37S rRNAs. More importantly, *MTR4* overexpression restored most of the 608 *rrp6*Δ-down-regulated mRNAs to wild-type-like levels; however, 29 mRNAs remained low or decreased further (Table 3). This suggests that persistent down-regulation of these mRNAs could cause the residual growth difference between *rrp6*Δ cells overexpressing *RRP6* and *MTR4*.

DISCUSSION

To understand why the *rrp6*Δ strain grows slowly, we identified high-copy-number extragenic suppressors on plates at 37°C and in liquid at 30°C. The liquid screen exploited a novel microarray method called MES, designed to complement the more traditional plate screen approach. MES identified the RNA-processing genes *LOS1* and *NAB6*, as well as the genes encoding the 3′-to-5′ exonucleases *REX1* to *-3*. A traditional plate screen also identified *REX1* and *REX3*, as well as genes encoding the exosome-associated factors *MTR4* and *DIS3*. By comparing the abilities of these suppressors to rescue at 30°C and 37°C on plates and in liquid, we found that some suppressors are temperature specific: *LOS1* and *NAB6* rescue only at 30°C, and *DIS3* rescues only at 37°C. Microarray assays comparing the suppressor strains with the initial *rrp6*Δ strain indicated that the mRNA population is affected in the *rrp6*Δ strain at 30°C, as well as 37°C; the data suggest that different sets of mRNAs are growth rate limiting at the two temperatures. The assays also provide insight into the specificities of different exonucleases.

MES is an analytical method that identifies high-copy-number suppressors and enhancers by linking the biological activities of genes to altered growth rates; rapid growers in the population accumulate suppressor genes, whereas slow growers lead to decreases in the representation of enhancer genes. The use of mixed cultures and microarrays has the virtue of simultaneously identifying multiple categories of genetic interactors: genes with subtle, as well as strong, effects and enhancers, as well as suppressors. The method is general and can be used with any starting mutant or physiological condition that has a slow-growth phenotype. MES identified 15 suppressor and 7 enhancer regions of the *rrp6*Δ slow-growth phenotype; 7 and 6 of these were verified by PCR, respectively (Fig. 2D and data not shown). Most of the identified enhancers were not strain specific, almost certainly because they include genes that are universally toxic at high copy numbers (data not shown). In contrast, the suppressors were specific to *rrp6*Δ and were not identified in MES with other mRNA export-related slow-growth mutations, such as *mex67-5* (data not shown). Two of the suppressors that we identified, *NAB6* and *LOS1*, illustrate the capacity of MES to isolate subtle suppressors that would not be identified in a traditional plate screen. Neither *NAB6* nor *LOS1* rescues the growth of the *rrp6*Δ strain on plates at 37°C; on the contrary, they are strong enhancers at 37°C. The other identified suppressors, *REX1*, *REX2*, and *REX3*, are robust suppressors at both temperatures. We note that *MTR4* rescues the growth defects of the *rrp6*Δ strain at 30°C, but it was not identified by MES. Most false negatives are probably due to technical limitations (see Materials and Methods).

The viable *rrp6*Δ strain has a myriad of RNA-relevant defects, many of which are likely due to suboptimal exosome function in the absence of the nuclear Rrp6p subunit and/or to dedicated functions of Rrp6p. These include the 3′-end formation of snRNAs, snoRNAs, and 5.8S rRNA (1, 10, 19, 44). Aberrant 5.8S rRNA processing then indirectly affects the processing of other rRNAs, i.e., 23S, 21S, and 18S intermediates accumulate (2). Ribosome assembly could also be impacted by improper rRNA modification due to insufficient snoRNA activity. In any case, the *rrp6*Δ strain has a decrease in functional 60S ribosomal subunits (10).

RRP6 is also implicated in early mRNA biogenic events. It is essential for retaining improperly processed mRNA near transcription sites (24) and is widely distributed on actively transcribed genes in *S. cerevisiae* (23). Rrp6p or components of the nuclear exosome copurify with the poly(A) polymerase Pap1p, as well as the mRNP proteins Npl3p and Yra1p (11, 46). *RRP6* also interacts genetically with many other factors involved in transcription, mRNA processing, and mRNA export (31, 46). In *Drosophila melanogaster*, Rrp6p colocalizes on active chromatin with RNA Pol II and the Spt5/6 transcription factors (6). The proximity to active transcription sites in yeast, as well as other organisms, probably reflects a phylogenetically conserved role of Rrp6p and the nuclear exosome in modulating RNA Pol II transcription or nascent mRNA processing.

Surprisingly, there are more mRNAs that decrease than that increase in the *rrp6*Δ strain: at 30°C, there are 13 mRNAs more than 10-fold down-regulated and only 3 more than 10-fold up-regulated (data not shown; see Table S2 in the supplemental material). At 37°C, the difference is more dramatic, with 608 mRNAs more than 10-fold down and only 83 mRNAs more than 10-fold up (Fig. 5 and data not shown). There is no obvious mechanistic explanation that directly links a decrease in exosome activity to an mRNA decrease, suggesting that the effect is indirect. A simple explanation we favor is that the large increase in nuclear poly(A) titrates essential mRNP factors, leading to decreased transport or stability of some mRNA species. Consistent with this explanation, Hieronymus and colleagues reported that both bulk polyadenylated RNA and a specific mRNA species accumulate in the nucleus in *rrp6*Δ cells (23).

MTR4, *DIS3*, *REX1*, *REX2*, and *REX3* may increase or partially complement defective exosome function or a missing independent activity of Rrp6p. Only excess Rex2p was able to partially restore both 5.8S rRNA and snoRNA processing when overexpressed (Fig. 4). This suggests that *MTR4*, *DIS3*, *REX1*, and *REX3* do not improve the growth rate of the *rrp6*Δ strain by restoring stable RNA processing. Additional observations support this conclusion and suggest that there is an adequate supply of most, if not all, of the stable RNA species, despite the striking increase in their polyadenylation. For example, we do not see any specific decrease in intron-containing mRNAs at 30°C or 36°C, suggesting that there is a sufficient level of functional splicing snRNAs. To test for overall deficiencies in ribosome assembly and translation, we examined the kinetics of heat shock protein synthesis in the *rrp6*Δ strain and found it to be identical to that of the wild type (data not shown). All of these observations suggest that snRNA, snoRNA, and rRNA processing are not growth rate limiting in the *rrp6*Δ strain, consistent with previous work (2, 37).

Despite their inability to rescue some RNA-processing defects, *MTR4*, *DIS3*, and *REX3* can reduce the levels of poly(A)-stable RNAs (Fig. 5 and 7), suggesting that they can stimulate the degradation of Trf4p-produced poly(A)-stable RNAs. It is possible that these suppressors modulate the growth rate by reducing the total level of poly(A)-stable RNA in the nucleus.

Although *MTR4* overexpression also rescues most of the mRNA defects of the *rrp6*Δ strain at 36°C, there is a small group of mRNAs that remain low and accompany the residual growth rate effect (Table 3). Given that growth is largely corrected, one might have anticipated a different result, namely, a substantial but incomplete rescue of all mRNA species. This suggests that the levels of some mRNA species are the cause of slow growth rather than just its consequence, with different RNAs being growth rate limiting at 36°C and at 30°C. mRNAs that are not rescued by *MTR4* overexpression are perhaps unusually sensitive to poly(A) titration or specifically require Rrp6p for transcription and/or processing. A larger set of affected mRNAs and/or more severe inhibition is probably responsible for the more severe growth defects (and lethality) of the *rrp6*Δ strain at 36°C than at 30°C. This presumably reflects a more severe exosome deficiency at higher temperature and perhaps a larger nuclear pool of poly(A)-stable RNAs.

A focus on individual Pol II mRNAs and translation is also indicated by the two MES growth suppressors, *LOS1* and *NAB6*. Neither Los1p nor Nab6p overexpression can restore 5.8S rRNA or snR38 processing at 30°C or 37°C. In addition, these two suppressors are much less effective at lowering overall poly(A)-stable RNA levels. Indeed, the overall level of poly(A)-stable RNAs [as calculated by summing all of the poly(A)-stable and CUT signals from Affymetrix arrays] is not affected with Nab6p overexpression and actually increases with Los1p overexpression (data not shown), despite decreases in the levels of a subset of the poly(A)-stable RNAs by both Los1p and Nab6p (Fig. 5). Because the microarray analyses of these strains indicate that increased growth at 30°C is accompanied by increases in specific mRNAs, we favor the notion that Los1p and Nab6p increase protein synthesis of mRNAs that are growth limiting for the *rrp6*Δ strain.

Based on its known role as a tRNA transporter, overexpressed Los1p may increase protein synthesis by increasing the cytoplasmic transport of some tRNAs. Because excess exportin T (the Los1p ortholog in higher eukaryotes) has been shown to export improperly processed tRNAs to the cytoplasm (7), excess Los1p might actually function by reducing the putative titration effect of excess nuclear poly(A) tRNAs.

The function of Nab6p is more enigmatic, because *NAB6* overexpression partially restores the levels of snRNAs and rRNAs. However, there are multiple indications that Nab6p is more directly involved in mRNA metabolism (Fig. 6 and Table 2). Nab6p binds to polyadenylated RNA (Fig. 6), interacts genetically with mRNA 3′-end processing factors (data not shown), copurifies with the nuclear cap-binding protein Cbp20p, and is found in complexes containing other translation factors, such as EIF4G (Tif4631 and TIF4632) (13). These results suggest that Nab6p may be involved in the processing, export, stability, or translatability of a subset of mRNAs that are growth limiting in the *rrp6*Δ strain at 30°C.

The difference between Los1p and Nab6p on the one hand and the rest of the suppressors on the other is further highlighted by their different effects at 30°C versus 37°C. Los1p and Nab6p promote growth at 30°C (the selection conditions for identifying the two suppressors) but inhibit growth and viability at 37°C. Los1p is also the only suppressor that increases the total levels of poly(A)-stable RNAs in the cell at 30°C (data not shown). At 36°C, the levels of poly(A)-stable RNAs increase at least twofold in the *rrp6*Δ strain (Fig. 7 and data not shown). When Los1p is overexpressed in this background, the levels of poly(A)-stable RNAs could rise even higher and be more toxic. This hypothesis is supported by fluorescence in situ hybridization experiments showing an increase in oligo(dT) staining in the nuclei of *rrp6*Δ cells overexpressing Los1p (data not shown). Alternatively, the abilities of Los1p and Nab6p to stimulate the synthesis of a subset of proteins could have a deleterious effect at 36°C, because it occurs at the expense of other proteins that are now limiting.

In summary, our data suggest that aberrant mRNA metabolism is most likely responsible for the slow-growth phenotype of the *rrp6*Δ strain. In addition, we anticipate that the MES approach will have wide application beyond suppressor and enhancer screening in yeast, as only minor modifications should be required for its use in mammalian systems.

ACKNOWLEDGMENTS

We thank colleagues in the Rosbash and Jensen laboratories, as well as former colleagues K. Dower and N. Kuperwasser, for helpful suggestions and encouragement. We are particularly grateful to Sebastian Kadener for help with the Affymetrix microarray analysis. We thank B. Goode for providing the *arp2-1* mutant strain (Y721).

The work was supported in part by grants from the NIH (GM23549) to M.R. and from the Danish National Research Foundation and the Novo Nordisk Foundation to T.H.J. K.A. was partially supported by an NIH postdoctoral fellowship (GM66640).

REFERENCES

1. **Allmang, C., J. Kufel, G. Chanfreau, P. Mitchell, E. Petfalski, and D. Tollervey.** 1999. Functions of the exosome in rRNA, snoRNA and snRNA synthesis. EMBO J. **18:**5399–5410.
2. **Allmang, C., P. Mitchell, E. Petfalski, and D. Tollervey.** 2000. Degradation of ribosomal RNA precursors by the exosome. Nucleic Acids Res. **28:**1684–1691.
3. **Allmang, C., E. Petfalski, A. Podtelenikov, M. Mann, D. Tollervey, and P. Mitchell.** 1999. The yeast exosome and human PM-Scl are related complexes of 3′-5′ exonucleases. Genes Dev. **13:**2148–2158.
4. **Anderson, J. S., and R. P. Parker.** 1998. The 3′ to 5′ degradation of yeast mRNAs is a general mechanism for mRNA turnover that requires the SKI2 DEVH box protein and 3′ to 5′ exonucleases of the exosome complex. EMBO J. **17:**1497–1506.
5. **Anderson, J. T., S. M. Wilson, K. V. Datar, and M. S. Swanson.** 1993. NAB2: a yeast nuclear polyadenylated RNA-binding protein essential for cell viability. Mol. Cell. Biol. **13:**2730–2741.
6. **Andrulis, E. D., J. Werner, A. Nazarian, H. Erdjument-Bromage, P. Tempst, and J. T. Lis.** 2002. The RNA processing exosome is linked to elongating RNA polymerase II in *Drosophila*. Nature **420:**837–841.
7. **Arts, G. J., S. Kuersten, P. Romby, B. Ehresmann, and I. W. Mattaj.** 1998. The role of exportin-t in selective nuclear export of mature tRNAs. EMBO J. **17:**7430–7441.
8. **Botstein, D., S. C. Falco, S. E. Stewart, M. Brennan, S. Scherer, D. T. Stinchcomb, K. Struhl, and R. W. Davis.** 1979. Sterile host yeasts (SHY): a eukaryotic system of biological containment for recombinant DNA experiments. Gene **8:**17–24.
9. **Bousquet-Antonelli, C., C. Presutti, and D. Tollervey.** 2000. Identification of a regulated pathway for nuclear pre-mRNA turnover. Cell **102:**765–775.
10. **Briggs, M. W., K. T. Burkard, and J. S. Butler.** 1998. Rrp6p, the yeast homologue of the human PM-Scl 100-kDa autoantigen, is essential for efficient 5.8 S rRNA 3′ end formation. J. Biol. Chem. **273:**13255–13263.
11. **Burkard, K. T., and J. S. Butler.** 2000. A nuclear 3′-5′ exonuclease involved in mRNA degradation interacts with poly(A) polymerase and the hnRNA protein Npl3p. Mol. Cell. Biol. **20:**604–616.
12. **Butler, J. S.** 2002. The yin and yang of the exosome. Trends Cell Biol. **12:**90–96.
13. **Colot, H. V., F. Stutz, and M. Rosbash.** 1996. The yeast splicing factor MUD13 is a commitment complex component and corresponds to CBP20, the small subunit of the nuclear cap-binding complex. Genes Dev. **10:**1699–1708.
14. **Das, B., J. S. Butler, and F. Sherman.** 2003. Degradation of normal mRNA in the nucleus of *Saccharomyces cerevisiae*. Mol. Cell. Biol. **23:**5502–5515.
15. **Das, B., S. Das, and F. Sherman.** 2006. Mutant LYS2 mRNAs retained and degraded in the nucleus of *Saccharomyces cerevisiae*. Proc. Natl. Acad. Sci. USA **103:**10871–10876.
16. **Davis, C. A., and M. Ares, Jr.** 2006. Accumulation of unstable promoter-associated transcripts upon loss of the nuclear exosome subunit Rrp6p in *Saccharomyces cerevisiae*. Proc. Natl. Acad. Sci. USA **103:**3262–3267.
17. **de la Cruz, J., D. Kressler, D. Tollervey, and P. Linder.** 1998. Dob1p (Mtr4p) is a putative ATP-dependent RNA helicase required for the 3′ end formation of 5.8S rRNA in *Saccharomyces cerevisiae*. EMBO J. **17:**1128–1140.
18. **Egecioglu, D. E., A. K. Henras, and G. F. Chanfreau.** 2006. Contributions of Trf4p- and Trf5p-dependent polyadenylation to the processing and degradative functions of the yeast nuclear exosome. RNA **12:**26–32.
19. **Fatica, A., M. Morlando, and I. Bozzoni.** 2000. Yeast snoRNA accumulation relies on a cleavage-dependent/polyadenylation-independent 3′-processing apparatus. EMBO J. **19:**6218–6229.
20. **Gentleman, R. C., V. J. Carey, D. M. Bates, B. Bolstad, M. Dettling, S. Dudoit, B. Ellis, L. Gautier, Y. Ge, J. Gentry, K. Hornik, T. Hothorn, W. Huber, S. Iacus, R. Irizarry, F. Leisch, C. Li, M. Maechler, A. J. Rossini, G. Sawitzki, C. Smith, G. Smyth, L. Tierney, J. Y. Yang, and J. Zhang.** 2004. Bioconductor: open software development for computational biology and bioinformatics. Genome Biol. **5:**R80.
21. **Grosshans, H., G. Simos, and E. Hurt.** 2000. Transport of tRNA out of the nucleus—direct channeling to the ribosome? J. Struct. Biol **129:**288–294.
22. **Guthrie, C., and G. R. Fink.** 1991. Guide to yeast genetics and molecular biology. Methods Enzymol. **194:**389–398.
23. **Hieronymus, H., M. C. Yu, and P. A. Silver.** 2004. Genome-wide mRNA surveillance is coupled to mRNA export. Genes Dev. **18:**2652–2662.
24. **Hilleren, P., T. McCarthy, M. Rosbash, R. Parker, and T. H. Jensen.** 2001. Quality control of mRNA 3′-end processing is linked to the nuclear exosome. Nature **413:**538–542.
25. **Jensen, T. H., J. Boulay, J. R. Olesen, J. Colin, M. Weyler, and D. Libri.** 2004. Modulation of transcription affects mRNP quality. Mol. Cell **16:**235–244.
26. **Jensen, T. H., J. Boulay, M. Rosbash, and D. Libri.** 2001. The DECD box putative ATPase Sub2p is an early mRNA export factor. Curr. Biol. **11:**1711–1715.
27. **Kadaba, S., A. Krueger, T. Trice, A. M. Krecic, A. G. Hinnebusch, and J. Anderson.** 2004. Nuclear surveillance and degradation of hypomodified initiator $tRNA^{Met}$ in *S. cerevisiae*. Genes Dev. **18:**1227–1240.
28. **Kuai, L., B. Das, and F. Sherman.** 2005. A nuclear degradation pathway controls the abundance of normal mRNAs in *Saccharomyces cerevisiae*. Proc. Natl. Acad. Sci. USA **102:**13962–13967.
29. **Kuai, L., F. Fang, J. S. Butler, and F. Sherman.** 2004. Polyadenylation of rRNA in *Saccharomyces cerevisiae*. Proc. Natl. Acad. Sci. USA **101:**8581–8586.
30. **LaCava, J., J. Houseley, C. Saveanu, E. Petfalski, E. Thompson, A. Jacquier, and D. Tollervey.** 2005. RNA degradation by the exosome is promoted by a nuclear polyadenylation complex. Cell **121:**713–724.
31. **Libri, D., K. Dower, J. Boulay, R. Thomsen, M. Rosbash, and T. H. Jensen.** 2002. Interactions between mRNA export commitment, 3′-end quality control, and nuclear degradation. Mol. Cell. Biol. **22:**8254–8266.
32. **Midtgaard, S. F., J. Assenholt, A. T. Jonstrup, L. B. Van, T. H. Jensen, and D. E. Brodersen.** 2006. Structure of the nuclear exosome component Rrp6p reveals an interplay between the active site and the HRDC domain. Proc. Natl. Acad. Sci. USA **103:**11898–11903.
33. **Mitchell, P., E. Petfalski, R. Houalla, A. Podtelejnikov, M. Mann, and D. Tollervey.** 2003. Rrp47p is an exosome-associated protein required for the 3′ processing of stable RNAs. Mol. Cell. Biol. **23:**6982–6992.
34. **Mitchell, P., and D. Tollervey.** 2001. mRNA turnover. Curr. Opin. Cell Biol. **13:**320–325.
35. **Moreau, V., A. Madania, R. P. Martin, and B. Winson.** 1996. The *Saccharomyces cerevisiae* actin-related protein Arp2 is involved in the actin cytoskeleton. J. Cell Biol. **134:**117–132.
36. **Petfalski, E., T. Dandekar, Y. Henry, and D. Tollervey.** 1998. Processing of the precursors to small nucleolar RNAs and rRNAs requires common components. Mol. Cell. Biol. **18:**1181–1189.
37. **Phillips, S., and J. S. Butler.** 2003. Contribution of domain structure to the RNA 3′ end processing and degradation functions of the nuclear exosome subunit Rrp6p. RNA **9:**1098–1107.
38. **Puig, O., F. Caspary, G. Rigaut, B. Rutz, E. Bouveret, E. Bragado-Nilsson, M. Wilm, and B. Seraphin.** 2001. The tandem affinity purification (TAP) method: a general procedure of protein complex purification. Methods **24:**218–229.
39. **Russell, I., and D. Tollervey.** 1995. Yeast Nop3p has structural and functional similarities to mammalian pre-mRNA binding proteins. Eur. J. Cell Biol. **66:**293–301.
40. **Samanta, M. P., and S. Liang.** 2003. Predicting protein functions from redundancies in large-scale protein interaction networks. Proc. Natl. Acad. Sci. USA **100:**12579–12583.
41. **Torchet, C., C. Bousquet-Antonelli, L. Milligan, E. Thompson, J. Kufel, and D. Tollervey.** 2002. Processing of 3′-extended read-through transcripts by the exosome can generate functional mRNAs. Mol. Cell **9:**1285–1296.
42. **Vanacova, S., J. Wolf, G. Martin, D. Blank, S. Dettwiler, A. Friedlein, H. Langen, G. Keith, and W. Keller.** 2005. A new yeast poly(A) polymerase complex involved in RNA quality control. PLOS Biol. **3:**e189.
43. **van Hoof, A., P. Lennertz, and R. Parker.** 2000. Three conserved members of the RNase D family have unique and overlapping functions in the processing of 5S, 5.8S, U4, U5, RNase MRP and RNase P RNAs in yeast. EMBO J. **19:**1357–1365.
44. **van Hoof, A., P. Lennertz, and R. Parker.** 2000. Yeast exosome mutants accumulate 3′-extended polyadenylated forms of U4 small nuclear RNA and small nucleolar RNAs. Mol. Cell. Biol. **2:**441–452.
45. **Wyers, F., M. Rougemaille, G. Breard, J.-C. Rousselle, M.-E. Dufour, J. Boulay, F. Devaux, A. Namane, D. Libri, B. Séraphin, and A. Jacquier.** 2005. Cryptic Pol II transcript degradation by nuclear quality control pathway involving a new poly(A) polymerase. Cell **121:**725–737.
46. **Zenklusen, D., P. Vinciguerra, J. C. Wyss, and F. Stutz.** 2002. Stable mRNP formation and export require cotranscriptional recruitment of the mRNA export factors Yra1p and Sub2p by Hpr1p. Mol. Cell. Biol. **22:**8241–8253.